Anion of the formic acid dimer as a model for intermolecular proton transfer induced by a π^* excess electron

Rafał A. Bachorz
Department of Chemistry, Quantum Chemistry Group, Adam Mickiewicz University, Poznań 60-780, Poland and Chemical Sciences Division, Fundamental Sciences Directorate, Pacific Northwest National Laboratory, Richland, Washington 99352

Maciej Harańczyk, Iwona Dąbkowska, and Janusz Rak
Department of Chemistry, University of Gdańsk, Gdańsk 80-952, Poland

Maciej Gutowski[a)]
Chemical Sciences Division, Fundamental Sciences Directorate, Pacific Northwest National Laboratory, Richland Washington 99352

(Received 23 February 2005; accepted 9 March 2005; published online 20 May 2005)

The neutral and anionic formic acid dimers have been studied at the second-order Møller–Plesset and coupled-cluster level of theory with single, double, and perturbative triple excitations with augmented, correlation-consistent basis sets of double- and triple-zeta quality. Scans of the potential-energy surface for the anion were performed at the density-functional level of theory with a hybrid B3LYP functional and a high-quality basis set. Our main finding is that the formic acid dimer is susceptible to intermolecular proton transfer upon an excess electron attachment. The unpaired electron occupies a π^* orbital, the molecular moiety that accommodates an excess electron "buckles," and a proton is transferred to the unit where the excess electron is localized. As a consequence of these geometrical transformations, the electron vertical detachment energy becomes substantial, 2.35 eV. The anion is barely adiabatically unstable with respect to the neutral at 0 K. However, at standard conditions and in terms of Gibbs free energy, the anion is more stable than the neutral by +37 meV. The neutral and anionic dimers display different IR characteristics. In summary, the formic acid dimer can exist in two quasidegenerate states (neutral and anionic), which can be viewed as "zero" and "one" in the binary system. These two states are switchable and distinguishable. © *2005 American Institute of Physics*. [DOI: 10.1063/1.1899144]

I. INTRODUCTION

Proton transfer is one of the simplest and most fundamental reactions in chemistry. The most common kind of tautomerism in organic chemistry involves structures that differ in the point of attachment of hydrogen, and the keto-enol (imine-enamine) equilibrium involves proton transfer between carbon and oxygen (nitrogen) atoms. Intermolecular proton transfer is involved in the reactions of acids with bases, which, according to the Lowry–Brønsted theory, are substances that are proton donors and acceptors, respectively.[1,2] Proton transfer is involved in a variety of chemical and biological processes. Proton motion coupled with electron transfer is the basic mechanism of bioenergetic conversion.[3] Elucidation of various mechanisms of intermolecular proton transfer might be important to further our understanding of biophysical and materials science processes.

The intra- and intermolecular tautomerizations involving nucleic acid bases have long been suggested as critical steps in mutations of DNA.[4,5] Intramolecular proton-transfer reactions have been studied for both isolated and solvated nucleic acid bases.[6,7] Intermolecular single and double proton-transfer reactions have been studied for the dimers of nucleic acid bases in both their ground and excited electronic states.[8,9,10]

We have recently reported that hydrogen-bond complexes of a nucleic acid base (NB) with a weak acid (HA) can undergo an intermolecular proton transfer upon an excess electron attachment,

$$\mathrm{NB}\cdots\mathrm{HA}+\mathrm{e}^-\rightarrow\mathrm{HNB}^{\cdot}\cdots\mathrm{A}^-, \tag{1}$$

with the products being a radical of hydrogenated nucleic acid base $(\mathrm{HNB})^{\cdot}$ and a molecular anion A^-, which results from deprotonation of the weak acid HA. A striking feature found in a series of combined computational and photoelectron spectroscopy studies is that the proton transfer might be barrier-free, as in the complexes of uracil or thymine with glycine,[11,12] formic acid,[13] uracil with alanine,[14] weak inorganic acids,[15,16] alcohols,[17,18] and a non-Watson–Crick complex of adenine and thymine.[19] The intermolecular proton transfer may also encounter a small barrier, as in the Watson–Crick complex of guanine with cytosine.[8]

In this series of studies we discussed the occurrence of barrier-free proton transfer as an outcome of the interplay among the deprotonation energy of HA, protonation energy of NB^-, and the energy of intermolecular hydrogen bonds.[11–19] We recognized that the driving force for the pro-

[a)]Electronic-mail: maciej.gutowski@pnl.gov

TABLE I. The vapor pressure P(mm Hg) for some nucleic acid bases and formic acid at 473 K.

Compound	log P(mm Hg)
Cytosine	−2.92[20]
Tymine	−1.17[20]
Adenine	−1.62[21]
Formic acid	3.92[22]

ton transfer is to stabilize the excess electron, which is localized in an antibonding $\pi(\pi^*)$ orbital in the valence anion of a nucleic acid base.

The nucleic acid bases are not easily amenable to gas-phase studies. A large fraction of molecules of biological interest (nucleic acid bases, amino acids, etc.) have very low vapor pressures (see Table I), even at temperatures above 200 °C, and easily decompose at elevated temperatures. Ion sources, which are based on high-pressure electrical discharges or laser vaporization, usually deliver intense ion beams but rely on ionization processes which are not easily controlled and can induce important fragmentation processes.[23] Thus, fundamental studies of intermolecular tautomerizations induced by an excess electron would benefit from model systems that form strong hydrogen bonds but display a larger vapor pressure than nucleic acid bases. Formic acid is an attractive model system with a significant vapor pressure at standard conditions (see Table I). Radicals and ions of its monomer have been computationally studied by Yu *et al.*[24]

Here, we report that intermolecular proton transfer upon an excess electron attachment is not limited to complexes of nucleic acid bases with weak acids but is a common phenomenon in complexes bound by cyclic hydrogen bonds. With PA and PD denoting proton acceptor and donor sites, respectively, we have computationally identified this process for the anionic dimers of formic acid [Fig. 1(a)], formamide [Fig. 1(b)], and in a heterodimer of formic acid with formamide [Fig. 1(c)].

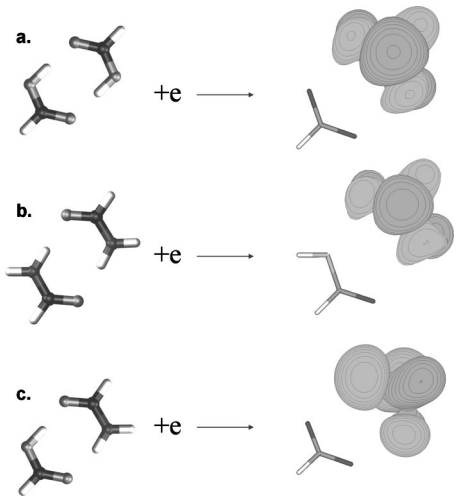

FIG. 1. Attachment of an excess π^* electron to a cyclic hydrogen-bonded cluster facilitates intermolecular proton transfer. The resulting complex is built of a buckled radical, which interacts through two hydrogen bonds with the anion of a deprotonated monomer: (a) formic acid dimer, (b) formamide dimer, and (c) formic acid-formamide.

The process has many similarities with that identified in anionic complexes of nucleic acid bases with weak acids: (i) the unpaired electron occupies a π^* orbital, (ii) the molecular unit that accommodates an excess electron "buckles" to suppress the antibonding interactions the excess electron is exposed to, (iii) a proton is transferred to the unit where the excess electron is localized—thus the unpaired electron is stabilized, (iv) the minimum energy structure for the anion is characterized by two strong hydrogen bonds between the radical $[R'\text{-}(\text{PD})_2]^{\cdot}$ and the anion $[R\text{-}(\text{PA})_2]^-$, (v) the electron vertical detachment energy (VDE) is substantial (1.6 eV $<$ VDE $<$ 2.4 eV), whereas the monomers involved, such as formic acid or formamide, do not bind an excess electron in a valence anionic state.

In this report we present our computational results for the anion of the formic acid dimer. The stability of the anionic $R'\text{-}(\text{PD})_2\cdots(\text{PA})_2\text{-}R$ structures, as a function of the proton affinity of the anion and the deprotonation energy of the neutral, will be described in a separate report and the results for $(\text{formamide})_2^-$ and $(\text{formic acid-formamide})^-$ will be presented there. An interesting feature of the formic acid dimer is that the minimum energy structure of the neutral is more stable than the minimum energy structure of the anion by only 2.7 kcal/mol, in terms of electronic energy, and by 0.4 kcal/mol after the inclusion of zero-point vibrational correction (0 K). Finally, at standard conditions (298 K, 1 atm) and in terms of Gibbs free energy, the anion is more stable than the neutral by +0.9 kcal/mol. Moreover, the anionic and neutral dimers differ drastically as to the structure as well as to their characteristic vibrational frequencies and their intensities. Thus, the formic acid dimer can exist in two quasidegenerate states (neutral and anionic), which can be viewed as "zero" and "one" in the binary system. These two states are switchable by the excess electron attachment and detachment. They are also distinguishable as they produce different electrostatic potential and differ in the geometry and spectroscopic characteristics.

II. METHODS

Initial calculations were performed at the density-functional level of theory with a hybrid exchange-correlation functional B3LYP[25,26,27] and 6-31++G** basis sets.[28] Final B3LYP calculations were performed with a polarized triple-ζ basis set (TZVP)[29] supplemented with valence diffuse functions (s and p for hydrogen, and s, p, and d for C and O) to better describe the electron charge distribution in anionic complexes (TZVP+). Exponents for the additional diffuse functions were as follows (atom, α_s, α_p, α_d: H, 0.04573, 0.222561; C, 0.04441, 0.02922, 0.196407; O, 0.08142, 0.04812, 0.249174). We verified that the addition of another set of diffuse functions changed the excess electron binding energy by less than 0.01 kcal/mol.

The vertical electron attachment energy is negative for an isolated formic acid molecule and for the formic acid dimer in its C_{2h} symmetry minimum-energy structure. Thus one needs to explore in which regions of the potential-energy

surface the dimer might support a bound anionic state. In other words, which intra- and intermolecular distortions are required to render the anionic state bound with respect to the neutral dimer and how large are energetic effects accompanying these distortions. These issues were explored using the B3LYP/TZVP+ model. The anionic potential-energy surface was scanned along selected degrees of freedom with the remaining geometrical parameters being optimized to minimize the total energy of the anionic complex (partial optimization with fixed selected variables). For the points on the resulting "paths," single-point calculations were performed for the neutral system to monitor whether the anion is vertically bound.

The most accurate electronic energies for the neutral and anionic complexes were calculated at the coupled-cluster level of theory with single, double, and perturbative triple excitations [CCSD(T)][30] at the optimal second-order Møller–Plesset (MP2) geometries. These calculations were performed with augmented correlation-consistent basis sets of double- and triple-ζ quality, which are denoted aug-cc-pVDZ and aug-cc-pVTZ, respectively.[31] The spin contamination was small in the unrestricted Hartree–Fock (UHF) and UB3LYP calculations for the anion (S^2 less than 0.759 for the UHF method), and thus the UMP2 optimized geometry for the anion is expected to be accurate. The open-shell CCSD(T) calculations were carried out at the R/UCCSD(T) level. In this approach, a restricted open-shell Hartree–Fock calculation was initially performed to generate the set of molecular orbitals and the spin constraint was relaxed in the coupled-cluster calculation.[32–34] The relative energies of the anion with respect to the neutral were first corrected for zero-point vibrations to derive the value of adiabatic electron affinity (AEA). Next, thermal corrections as well as the entropy terms, calculated at either the B3LYP or MP2 levels for $T=298$ K and $p=1$ atm in the harmonic oscillator-rigid rotor approximation, were included to derive the relative stability in terms of Gibbs free energy.

The DFT and MP2 calculations were performed with the GAUSSIAN 98[28] and NWCHEM codes,[35] while the CCSD(T) calculations with the MOLPRO code.[36] Molecular orbitals and structures were visualized with the MOLDEN program.[37]

III. RESULTS

A. Structures

The neutral formic acid dimer was thoroughly studied by many groups and we selected the same initial structures "*n*X" as those identified by Qian and Krimm,[38] and we apply their notation in Fig. S1(a).[39] The anionic structures determined in the course of geometry optimization initialized from the optimal geometry of the neutral structure *n*X will be labeled *a*X. The relative energies of the neutral and anionic structures, calculated with respect to the most stable C_s anion (*a*II), are displayed in Fig. S2.[39] To the best of our knowledge, the anionic dimer has not yet been studied and our calculations reveal that its most stable structure differs drastically from the most stable structure of the neutral (see Fig. 2). From here on we will discuss only the most stable neutral and anionic complexes, *n*II and *a*II, respectively, as other structures are much less stable.

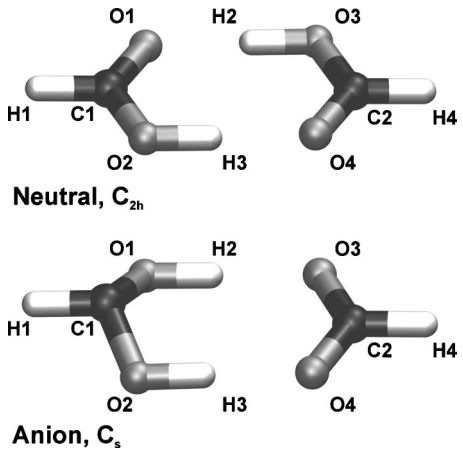

FIG. 2. The global minima for the neutral and anionic formic acid dimer.

The C_s anionic complex differs drastically from the C_{2h} neutral complex, see Scheme 1, Fig. 2, and Tables II and III. First, an intermolecular proton transfer occurred in the unit where the unpaired electron is localized. Second, the resulting radical is "buckled," and the extent of buckling will be measured by the values of the H1–C1–O1–O2 dihedral angle, ϑ. The buckling of the $R'(PD)_2$ unit in the anionic dimer is significant and both the B3LYP and MP2 methods predict that ϑ is ca. 132° (see Table III). This buckling is reminiscent of the buckling of the ring of nucleic acid bases upon an excess electron attachment. In all these cases the excess electron occupies a π^* orbital. The buckling alleviates the antibonding character of this orbital and stabilizes the anionic structure.

In addition to the intermolecular proton transfer and the buckling of the $R'(PD)_2$ unit, the neutral and anionic complex differ quantitatively with respect to some of the geometrical parameters (see Tables II and III). For instance the C1O2 distance is increased by ca. 0.05 Å in the anion at both the MP2 and B3LYP levels, which might be again related to the antibonding character of the single occupied orbital.

The hydrogen bonds in both the neutral and anionic dimer are practically linear as the O2–H3–O4 angle is always between 178° and 180°. One usually expects a shorter hydrogen bond in the ionic than the neutral complex. Sur-

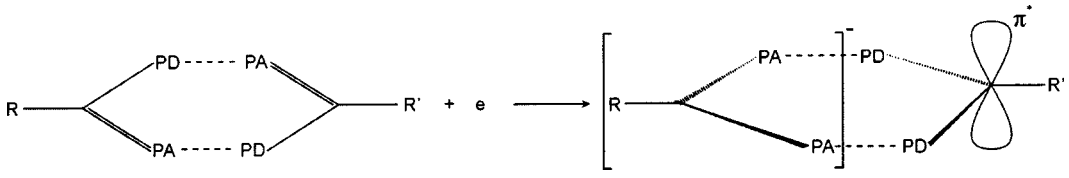

SCHEME 1. Intermolecular proton transfer induced by a π^* excess electron in a complex with cyclic hydrogen bonds.

TABLE II. Structural parameters for the C_{2h} symmetry neutral complex obtained at the B3LYP and MP2 levels of theory. Bond lengths in Å, angles in deg.

Parameter	B3LYP/TZVP+	MP2/aug-cc-pVDZ	MP2/aug-cc-pVTZ
Bond			
H1–C1	1.095	1.101	1.091
C1–O2	1.315	1.325	1.313
C1–O1	1.225	1.233	1.224
O2–H3	1.007	1.001	1.000
H3–O4	1.665	1.683	1.660
Angle			
H1–C1–O2	111.930	111.590	111.750
H1–C1–O1	121.730	122.090	121.940
O2–H3–O4	178.710	179.680	179.930
Dihedral angle			
H1–C1–O1–O2	180.000	180.000	180.000

prisingly, this is not true for the neutral and anionic formic acid dimer as the H3O4 distance in both cases is the same, within 0.02 Å.

B. Excess electron binding and stability of the anion

The formic acid monomer and the neutral C_{2h} dimer have negative vertical electron attachment energies (VAE). Not only valence but also dipole-bound anionic states[40] are not bound because the dipole moment of the monomer calculated at the B3LYP/TZVP+ level of theory is only 1.74 D, and the dimer has no dipole moment due to the C_{2h} symmetry. On the other hand, the electron vertical detachment energy (VDE), which is calculated at the equilibrium geometry of the anion, is significant and amounts to 2.35 eV at the CCSD(T)/aug-cc-pVTZ level of theory (see Table IV). A significant value of VDE is a consequence of intermolecular proton transfer to the unit, where the unpaired electron is localized. A negative value of VAE and a positive value of VDE are also characteristics of valence anionic states of canonical tautomers of nucleic acid bases, though their values

TABLE III. Structural parameters for the C_s symmetry anionic complex obtained at the B3LYP and MP2 levels of theory. Bond lengths in Å, angles in deg.

Parameter	B3LYP/TZVP+	MP2/aug-cc-pVDZ	MP2/aug-cc-pVTZ
Bond			
H1–C1	1.091	1.099	1.086
C1–O2	1.371	1.378	1.366
O2–H3	1.004	1.003	1.000
H3–O4	1.679	1.677	1.663
O4–C2	1.260	1.270	1.259
C2–H4	1.117	1.122	1.112
Angle			
H1–C1–O2	111.880	111.350	111.630
O2–H3–O4	178.530	177.680	177.790
O4–C2–H4	115.690	115.730	115.750
Dihedral angle			
H1–C1–O1–O2	132.870	131.070	131.860

TABLE IV. Electron vertical detachment energies (VDE) and adiabatic electron affinity (AEA), both in meV, determined at different levels of theory.

	VDE	AEA	AEA (without ZPVE)
B3LYP/TZVP	2500	122	28
B3LYP/TZVP+	2516	233	133
B3LYP/TZVP++	2501	234	132
MP2/aug-cc-pVDZ	2387	−87	−185
MP2/aug-cc-pVTZ	2351	−64[a]	−163
CCSD/aug-cc-pVDZ	2504	−37[a]	−136
CCSD/aug-cc-pVTZ	2469	−42[a]	−140
CCSD(T)/aug-cc-pVDZ	2377	−29[a]	−128
CCSD(T)/aug-cc-pVTZ	2351	−18[a]	−117

[a]Zero-point vibrational corrections determined at the MP2/aug-cc-pVDZ level.

of VDE are smaller than those for the anionic formic acid dimer and do not exceed 0.6 eV.[7,11,12,41] The value of VDE is overestimated at the B3LYP level when compared with the CCSD(T) result, which is also typical for anions of nucleic acid bases. The small discrepancy between the CCSD and the CCSD(T) results as well as the aug-cc-pVDZ and aug-cc-pVTZ results prompts us to conclude that the 2.35-eV value for VDE is both methodologically and basis-set converged (see Table IV).

The anion is barely adiabatically unstable with respect to the neutral at 0 K. At the CCSD(T)/aug-cc-pVTZ level, a contribution from electronic energies to the AEA is −117 meV (Table IV), but a contribution from the zero-point vibrational terms suppresses the instability to only −18 meV. Finally, at standard conditions and in terms of Gibbs free energy, the anion is more stable than the neutral by +37 meV. Clearly, the anion has softer modes than the neutral (see Tables S2 and S3),[39] and zero-point vibrational contributions and vibrational contributions to entropy increase the stability of the anion over the neutral.

The C_s symmetry R'-$(PD)_2\cdots(PA)_2$-R structure, which is the global minimum for the anion, is not a local minimum for the neutral dimer. A geometry optimization procedure on the potential-energy surface of the neutral dimer initiated from a slightly distorted R'-$(PD)_2\cdots(PA)_2$-R geometry converges without any barrier to the C_{2h} structure of the neutral, i.e., R'-(PA,PD)$\cdots$(PD,PA)-R. Thus an excess electron is required to stabilize the C_s R'-$(PD)_2\cdots(PA)_2$-R structure.

The lifetime of the adiabatically unbound anionic state, $(R'$-$(PD)_2\cdots(PA)_2$-$R)^-$, depends not only on the value of AEA but also on the magnitude of atomic displacements from the C_s minimum required to reach a crossing with the potential-energy surface of the neutral. The anionic potential-energy surface was scanned along the dihedral angle ϑ, with the remaining geometrical parameters being optimized at the B3LYP/TZVP+ level, and the results are presented in Fig. 3. On the second vertical axis we also report optimized values of the H2O3 distance, which is an indicator of whether the R'-$(PD)_2\cdots(PA)_2$-R or the R'-(PA,PD)$\cdots$(PD,PA)-R structure prevails.

In Fig. 3(a) we present the case with the angle ϑ being *decreased* from 180° to 115° and the geometry optimization for the anion initialized in the neighborhood of the C_{2h} ge-

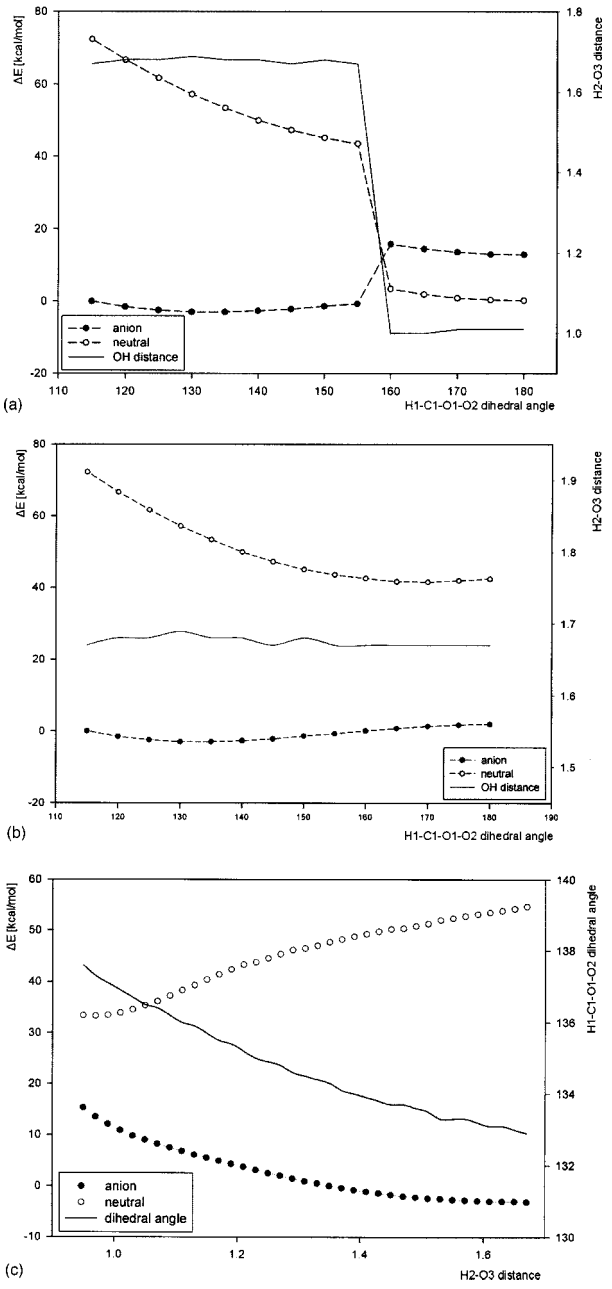

FIG. 3. Plots of the relative electronic energy of neutral and anionic dimers obtained at the B3LYP/TZVP+ level of theory in the course of partial geometry optimizations with fixed selected variables. The relative energies calculated with respect to the C_{2h} neutral. Bond lengths in Å, angles in deg. a) The angle H1–C1–O1–O2 was *decreased* from 180° to 115° and the H2–O3 distance was displayed on the second vertical axis, b) the angle H1–C1–O1–O2 was *increased* from 115° to 180° and the H2–O3 distance was displayed on the second vertical axis, c) the H2–O3 distance was changed between 0.9 and 1.7 Å and the dihedral angle H1–C1–O1–O2 was displayed on the second vertical axis.

ometry of the neutral. The optimized H2O3 distance does not exceed 1.05 Å for $160° \leqslant \vartheta \leqslant 180°$; thus the R'-$(PA,PD)\cdots(PD,PA)$-R structure prevails. The anion remains unbound for this range of ϑ. Since the basis set contains functions with very small exponents, the excess electron is distributed far away from the molecular core and the optimized structure of the anion resembles the structure of the neutral. With the angle ϑ further decreased, an intermolecular proton transfer occurs and the H2O3 distance exceeds

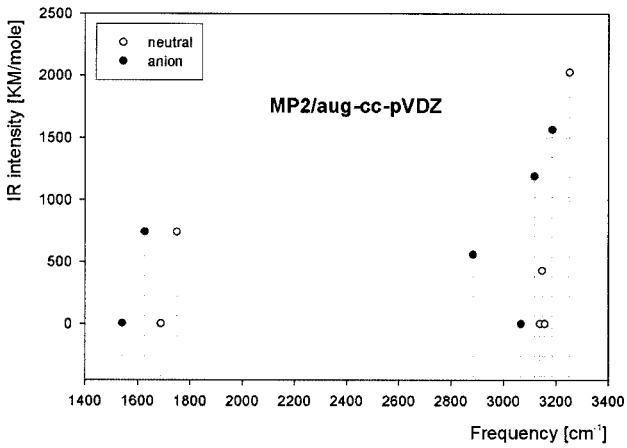

FIG. 4. Harmonic vibrational frequencies in the 1400–3400 cm^{-1} range and the corresponding IR intensities for the neutral and anionic dimer determined at the MP2/aug-cc-pVDZ level.

1.45 Å for $115° \leqslant \vartheta \leqslant 155°$. Thus the R'-$(PD)_2\cdots(PA)_2$-R structure prevails for this range of ϑ. Moreover, the anionic state becomes vertically bound with respect to the neutral as a consequence of intermolecular proton transfer.

In Fig. 3(b) we present the case with the angle ϑ being *increased* from 115° to 180° and the geometry optimization for the anion initialized in the neighborhood of the C_s geometry of the anion. The main finding is that the R'-$(PD)_2\cdots(PA)_2$-R structure is preserved even for ϑ close to 180°. The R'-$(PD)_2$ unit remains nonplanar even for ϑ equal to 180°, and the anion is vertically bound with respect to the neutral for the full range of ϑ. Apparently, the intermolecular proton transfer is sufficient to stabilize the anion.

In Fig. 3(c) we present the case with the H2O3 distance being changed between 0.95 and 1.67 Å. Thus both the R′-$(PA,PD)\cdots(PD,PA)$-R and the R'-$(PD)_2\cdots(PA)_2$-R structures are explored. All other geometrical parameters are optimized and the optimal values of ϑ are displayed on the second vertical axis. The anion remains vertically bound with respect to the neutral even for the values of the H2O3 distance as small as 1.0 Å and the values of ϑ remain within a narrow range $132° < \vartheta < 138°$. Apparently, the buckling of one of the monomers is sufficient to stabilize the anion.

C. IR spectra of the neutral and anionic dimer

The remaining question is whether the neutral and the anionic dimer can be discriminated on the basis of spectroscopic characteristics. The harmonic frequencies and IR intensities were calculated at the MP2/aug-cc-pVDZ and B3LYP/TZVP+ levels for the neutral monomer, neutral dimer, and anionic dimer, and the results are presented in Tables S1–S3.[39] We will concentrate here on a frequency range from 1400 to 3400 cm^{-1}, which covers the CO, CH, and OH stretching modes; see Fig. 4 for the MP2/aug-cc-pVDZ results. The modes with frequencies in a range of 1400–1800 cm^{-1} are dominated by the CO stretches and OHC bendings. These modes have very similar IR intensities for the neutral and the anion, but the anionic frequencies are smaller by more than 100 cm^{-1}. The modes with frequencies in a range of 2800–3300 cm^{-1} are dominated by the CH and

OH stretches, which are strongly coupled, in particular for the anion. Both the neutral and the anion have a mode with an IR intensity of ca. 500 KM/mole. The frequency for the anion is, however, red shifted by more than 250 cm^{-1}. The anionic dimer has two intense modes in a range of 3100–3200 cm^{-1}, whereas the neutral dimer has only one intense mode, which is at ca. 3250 cm^{-1}. We conclude that the neutral and anionic dimers differ significantly in IR characteristics.

IV. SUMMARY

The neutral and anionic formic acid dimer were studied at the second-order Møller–Plesset and coupled-cluster level of theory with single, double, and perturbative triple excitations with augmented, correlation-consistent basis sets of double- and triple-zeta quality. Scans of the potential-energy surface for the anion were performed at the density-functional level of theory with a hybrid B3LYP functional and a high-quality basis set.

Our main finding is that the formic acid dimer is susceptible to intermolecular proton transfer upon an excess electron attachment. The process has many similarities with intermolecular proton transfer which we have identified in the past in anionic complexes of nucleic acid bases with weak acids:[11–19] (i) the unpaired electron occupies a π^* orbital, (ii) the molecular unit that accommodates an excess electron "buckles" to suppress the antibonding interactions the excess electron is exposed to, (iii) a proton is transferred to the unit where the excess electron is localized—thus the unpaired electron is stabilized, (iv) the electron vertical detachment energy is substantial, 2.35 eV, whereas the formic acid monomer and the neutral dimer are characterized by negative values of vertical electron attachment energy.

The anion is barely adiabatically unstable with respect to the neutral at 0 K. At the CCSD(T)/aug-cc-pVTZ level, a contribution from electronic energies to the adiabatic electron affinity is −117 meV, but a contribution from the zero-point vibrational terms suppresses the instability to only −18 meV. Finally, at standard conditions and in terms of the Gibbs free energy, the anion is more stable than the neutral by +37 meV. The near degeneracy in stability for the neutral and the anion requires a serious geometrical relaxation within the anionic structure. First, a proton is transferred to a unit where the unpaired electron is localized. Second, the protonated subunit buckles to suppress the antibonding interactions the excess π^* electron is exposed to. The geometrical distortion from the neutral and the anion is more profound than in the case of the monomer of carbon dioxide.[42] Thus, we expect that the anionic formic acid dimer will have a significant lifetime.

The neutral and anionic dimers display different IR characteristics. In a range of 1400–1800 cm^{-1} (CO stretches and OHC bendings), the neutral and the anion have very similar IR intensities, but the anionic frequencies are smaller by more than 100 cm^{-1}. In a range of 2800–3300 cm^{-1} (CH and OH stretches), both the neutral and the anion have a mode with an IR intensity of ca. 500 KM/mole. The frequency of the anion is, however, red shifted by more than 250 cm^{-1}. The anionic dimer has two intense modes in a range of 3100–3200 cm^{-1}, whereas the neutral dimer has only one intense mode, which is at ca. 3250 cm^{-1}.

We conclude that the formic acid dimer can exist in two quasidegenerate states (neutral and anionic), which can be viewed as zero and one in the binary system. These two states are switchable by the excess electron attachment and detachment. They are also distinguishable as they produce different electrostatic potential and differ in the geometry and spectroscopic characteristics.

ACKNOWLEDGMENTS

The discussions with Professor Kit Bowen are gratefully acknowledged. This work was supported by the US DOE Office of Biological and Environmental Research, Low Dose Radiation Research Program, and the Laboratory Directed Research and Development Program at the PNNL (M.G.) as well as by the Polish State Committee for Scientific Research (KBN) Grant No. 4 T09A 012 24 (J.R. and M.H.). I.D. is a holder of a Foundation for Polish Science (FNP) award. Computing resources were available through: (i) a Computational Grand Challenge Application grant from the Molecular Sciences Computing Facility (MSCF) in the Environmental Molecular Sciences Laboratory, (ii) the National Energy Research Scientific Computing Center (NERSC), and (iii) the Academic Computer Center in Gdańsk (TASK). The MSCF is funded by DOE's Office of Biological and Environmental Research. PNNL is operated by Battelle for the U.S. DOE under Contract No. DE-AC06-76RLO 1830.

[1] T. M. Lowry, Chem. Ind. **42**, 43 (1923).
[2] J. N. Brønsted, Recl. Trav. Chim. Pays-Bas **42**, 7180 (1923).
[3] C. J. Chang, M. C. Y. Chang, N. H. Damrauer, and D. G. Nocera, Biochim. Biophys. Acta **1655**, 13 (2004).
[4] P. O. Lowdin, Rev. Mod. Phys. **35**, 724 (1963).
[5] I. Dąbkowska, M. Gutowski, and J. Rak, J. Am. Chem. Soc. **127**, 2238 (2005).
[6] P. Hobza and J. Sponer, Chem. Rev. (Washington, D.C.) **99**, 3247 (1999).
[7] M. Harańczyk and M Gutowski, J. Am. Chem. Soc. **127**, 699 (2005).
[8] X. Li, Z. Cai and M. D. Sevilla, J. Phys. Chem. A **105**, 10115 (2001).
[9] Y. Podolan, L. Gorb, and J. Leszczynski, Int. J. Mol. Sci. **4**, 410 (2003).
[10] T. Schultz, E. Samoylova, W. Radloff, I. V. Hertel, A. L. Sobolewski, and W. Domcke, Science, **306**, 1765 (2004).
[11] M. Gutowski, I. Dąbkowska, J. Rak, S. Xu, J. M. Nilles, D. Radisic, and K. H. Bowen, Jr., Eur. Phys. J. D **20**, 431 (2002).
[12] I. Dąbkowska, J. Rak, M. Gutowski, J. M. Nilles, S. T. Stokes, D. Radisic, and K. H. Bowen, Jr., Phys. Chem. Chem. Phys. **6**, 4351 (2004).
[13] M. Harańczyk, I. Dąbkowska, J. Rak, M. Gutowski, J. M. Nilles, S. T. Stokes, D. Radisic, and K. H. Bowen, Jr., J. Phys. Chem. A **108**, 6919 (2004).
[14] I. Dąbkowska, J. Rak, M. Gutowski, J. M. Nilles, D. Radisic, and K. H. Bowen, Jr., J. Chem. Phys. **120**, 6064 (2004).
[15] M. Harańczyk, R. Bachorz, J. Rak, M. Gutowski, J. M. Nilles, S. T. Stokes, D. Radisic, and K. H. Bowen, Jr., J. Phys. Chem. B **107**, 7889 (2003).
[16] M. Harańczyk, J. Rak, M. Gutowski, D. Radisic, S. T. Stokes, and K. H. Bowen, Jr., Isr. J. Chem. **44**, 157 (2004).
[17] M. Harańczyk and M. Gutowski, Internet Electronic Journal of Molecular Design **3**, 368 (2004); http://www.biochempress.com
[18] M. Harańczyk, J. Rak, M. Gutowski, D. Radisic, S. T. Stokes, and K. H. Bowen, J. Phys. Chem. B (submitted).
[19] D. Radisic, K. H. Bowen, Jr., I. Dąbkowska, P. Storoniak, J. Rak, and M. Gutowski, J. Am. Chem. Soc. (in press).
[20] D. Ferro, L. Bencivenni, R. Teghil, and R. Mastromarino, Thermochim. Acta **42**, 75 (1980).
[21] L. B. Clark, G. G. Peschel, and I. Tinoco, J. Phys. Chem. **69**, 3615 (1965).

[22]*Chemical Properties Handbook*, edited by C. L. Yaws (McGraw-Hill, New York, 1999), http://www.knovel.com/knovel2/
[23]C. Desfrancois, S. Carles, and J. P. Schermann, Chem. Rev. (Washington, D.C.) **100**, 3943 (2000).
[24]D. Yu, A. Rauk, and D. A. Armstrong, J. Chem. Soc., Perkin Trans. 2 **1994**, 2207.
[25]A. D. Becke, Phys. Rev. A **38**, 3098 (1988).
[26]A. D. Becke, J. Chem. Phys. **98**, 5648 (1993).
[27]C. Lee, W. Yang, and RG. Paar, Phys. Rev. B **37**, 785 (1988).
[28]M. J. Frisch *et al.*, GAUSSIAN 98 (Revision A.11), Gaussian, Inc., Pittsburgh, PA, 2001.
[29]N. Godbout, D. R. Salahub, J. Andzelm, and E. Wimmer, Can. J. Chem. **70**, 560 (1992).
[30]P. R. Taylor, in *Lecture Notes in Quantum Chemistry II*, edited by B. O. Roos (Springer, Berlin, 1994).
[31]R. A. Kendall, T. H. Dunning, Jr., and R. J. Harrison, J. Chem. Phys. **96**, 6796 (1992).
[32]M. Rittby and R. J. Bartlett, J. Phys. Chem. **92**, 3033 (1988).
[33]P. J. Knowles, C. Hampel, and H.-J. Werner, J. Chem. Phys. **99**, 5219 (1994).
[34]J. J. O. Deegan and P. J. Knowles, Chem. Phys. Lett. **227**, 321 (1994).
[35]T. P. Straatsma *et al.*, NWCHEM, a computational chemistry package for parallel computers, Version 4.6, Pacific Northwest National Laboratory, Richland, WA, 2004.
[36]H.-J. Werner *et al.*, MOLPRO, a package of *ab initio* programs, School of Chemistry, University of Birmingham, Birmingham, U.K., 2003.
[37]G. Schaftenaar and J. H. Noordik, J. Comput.-Aided Mol. Des. **14**, 123 (2000).
[38]W. Qian and S. Krimm, J. Phys. Chem. A **105**, 5046 (2001).
[39]See EPAPS Document No. E-JCPSA6-122-313521 for the relative stability of the various structures of the neutral and anionic formic acid dimer determined at the B3LYP/6−31++G** level, and of the vibrational frequencies and IR intensities of the formic acid monomer and the neutral and anionic formic acid dimer determined at the MP2 and B3LYP levels of theory. A direct link to this document may be found in the online article's HTML reference section. The document may also be reached via the EPAPS homepage (http://www.aip.org/pubservs/epaps.html) or from ftp.aip.org in the directory /epaps. See the EPAPS homepage for more information.
[40]M. Gutowski, K. D. Jordan, and P. Skurski, J. Phys. Chem. A **102**, 2624 (1998).
[41]K. Aflatooni, G. A. Gallup, and P. D. Burrow, J. Phys. Chem. A **102**, 6205 (1998).
[42]A. Rauk, D. A. Armstrong, and D. Yu, Int. J. Chem. Kinet. **26**, 7 (1994).